



Research paper

State Space Modeling and Sliding Mode Current Control of the Grid Connected Multi-Level Flying Capacitor Inverters

N. Ghaffari¹, A. Zakipour^{1,*}, M. Salimi²

¹Department of Electrical Engineering, Arak University of Technology (AUT), Arak, Iran.

²Department of Electrical Engineering, Ardabil Branch, Islamic Azad University, Ardabil, Iran.

Article Info

Article History:

Received 22 July 2020
Reviewed 15 September 2020
Revised 02 November 2020
Accepted 02 January 2021

Keywords:

Multi-level inverters
Grid connected inverter
Sliding mode control
Nonlinear control
Lyapunov stability
Active power filter

*Corresponding Author's Email
Address:

zakipour@arakut.ac.ir

Abstract

Background and Objectives: In this paper, a novel approach for regulation of the output current in the grid-connected three-level flying capacitor inverter is presented by using the sliding mode (SM) method. In the proposed method, it is possible to control the active and reactive components of the inverter output current independently, and therefore it can be employed for grid connection of the renewable energy resources or for harmonic and reactive power compensation of the local loads. The designed controller uses an external loop to control the voltage of the inverter DC link and has a constant switching frequency. The stability of the proposed method has also been proved by using the Lyapunov stability theory. The simulation results show that in different operating conditions, the proposed controller has a stable and robust response.

Methods: Grid-connected three-level flying capacitor inverter is modeled by using averaged state space technique. Considering nonlinearity of the obtained model, an equivalent SM controller is developed for output current control of the multilevel grid connected inverter. To improve robustness and stability of the system against uncertainty of model parameters, a nonlinear component is added to the equivalent controller.

Results: The proposed controller enjoys very fast dynamic response, so it can be employed in wide ranges of application e.g. reactive compensation and harmonic mitigation modes. In active power filtering operation, it is able to eliminate harmonic components of the grid from 20.61% to 1.34% which is compatible with IEEE and IEC standards.

Conclusion: The stability of the proposed method has also been proved by using the Lyapunov stability theory. The simulation results show that in different operating conditions, the proposed controller has a stable and robust response.

©2021 JECEI. All rights reserved.

Introduction

Application of the grid-connected inverters has increased significantly in recent years [1]. For example, in photovoltaic power plants, these inverters are used to inject active power generated by solar panels into the grid. In flexible AC transmission systems [2], grid-

connected inverters are used for load and line compensation through reactive power exchange. Also in active power filters [3], these power electronics converters are employed for harmonic compensation of the nonlinear loads. Other applications include wind power conversion systems [4], solid-state transformers

[5], connecting electric vehicles to the grid for peak shaving [6], and more.

From power circuit topology viewpoint, the standard H-bridge voltage source inverter is one of the most widely used power electronics converters which are employed in grid connected three-phase and single-phase systems. However, other topologies have been proposed in recent years to improve the performance of grid-connected systems. For example, the use of impedance and quasi-impedance source inverters for efficiency improvement of power converters in renewable energy systems is reported [7]. Also, to reduce switching losses and improve inverter output power quality, application of the multilevel inverters has been suggested in [8]. It is well-known that one of the main applications of the multilevel inverters is reduction of the switching harmonics and improvement of the output power quality. In fact, if IGBT based multilevel inverter with fast PWM switching is used, harmonic components of the inverter output current can be reduced significantly.

One of the main challenges in design and implementation of the grid-connected inverters is synchronizing of the inverter output voltage with the grid power. In such a case, exchanged power be controlled by adjusting the amplitude as well as the angle of the inverter output voltage vector [9]. However, in such a method, a small error in the output voltage phase can lead to a significant error in amount of the power which is exchanged between the inverter and the grid. For this reason, intrinsic delay in electronic systems such as analog-to-digital converters, mathematical calculations, and current and voltage sensors essentially complicates design of the closed-loop system. On the other hand, since the grid is essentially a voltage source, therefore, by controlling the output current of the inverter, the exchanged power between the grid and the inverter can be indirectly adjusted [10]. During output current control of the voltage source inverters, delay in response of electronic systems doesn't affect the amplitude of the current directly and therefore, it is more useful than direct control of the output voltage.

Briefly, output current and power control is one of the main blocks of inverters which are connected to the grid. If the reference values of the controller change sharply due to variation of the local load or DC input source, it is obvious that the dynamic response of the closed-loop controller must be fast enough to meet the system requirements of the grid-connected inverter. Also, considering the nonlinear nature of power electronics converters, basically the linear and conventional control methods will be able to stabilize and control the closed loop system only in a small range of the changes. For this reason, application of modern

and nonlinear methods for the current control of the grid connected voltage source inverters is proposed. For instance, adaptive [11], robust [12], backstepping [3], passivity-based [13], Lyapunov-based [14] controllers are used widely in closed loop control of the power electronics converters.

Among the mentioned methods, sliding mode (SM) controller is employed widely in power electronics converters [15]. Its main advantages are simplicity of the practical implementation, fast dynamic response and robustness to system uncertainties [16]. Also, in recent years, attempts have been made to eliminate the major drawbacks of the SM method, such as switching frequency changes, steady-state error, and chattering, by using the equivalent SM approach and in recent years, application of the SM controllers in grid-connected inverters has increased significantly. Also for mitigation of the chattering problem, combined PI and SM technique can be employed [17] where variable structure control approach is designed for shunt compensation of the local loads. To improve robustness and stability of the closed loop system, a SM controller in combination with conventional PI method is used in the final control law of the proposed method. During transient conditions, the PI controller is dominant and the gains of the linear controller should be tuned to meet the desired transient response characteristic. On the other hand, the sliding mode block determines steady-state behavior of the system. Briefly, in order to achieve desired response of the closed loop system and eliminate chattering problem, gains for the linear PI and SM controllers should be selected properly. The SM is employed for grid connection of the cascaded doubly fed induction generators [18]. Two sliding surfaces are defined for closed loop control of the active and reactive power components. Compared with conventional vector control, it is shown that the SM method is more robust against model uncertainties and enjoys better dynamic response. However, in the proposed method, stability of the closed loop system under different operating conditions has not been investigated.

In order to reduce the output current error of the inverter and thus improve the total harmonic distortion (THD) coefficient of the power system, in [19] a multi-resonance SM controller is used in the grid connected inverters. In this case, the performance of the system in compensating for the high order harmonics is increased. To reduce THD, in sliding surface the proposed controller, several resonant components from the grid current error are employed which complicates design of the controller and its practical implementation.

To improve the power quality in power distribution networks and reduce power losses in electrical equipment, the Integral SM method has been used to

control the output current of the grid connected inverter in [20]. A fourth-order band pass digital filter is used to extract the harmonic components and define the reference values of the closed-loop control system. Since the main component of the output current in the proposed method is regulated by using a linear PI controller, it can be concluded that the chattering will be significantly reduced. However, such an approach does not guarantee the overall stability of the controller over a wide range of output current changes. Also, for controlling of the fundamental current component, two PI blocks are used for calculation of the reference value and inverter amplitude modulation (control effort). As a result, the proposed closed-loop system has a cascade structure that cannot have a fast dynamic response and will lead to a steady-state error when compensating for high-order harmonic components. Also, a double band hysteresis SM controller is proposed for parallel operation of the active power filters with LCL coupling in reference [21]. Despite the fast dynamic response, the switching instances in the proposed method are determined by comparison of the slip surface in a hysteresis band. Hence, inverter switching frequency cannot be completely constant due to variation of the grid voltage. This issue results in injection of the undesired low-order harmonic components and deteriorates the THD of the grid current. However, if the hysteresis-based SM is replaced with equivalent controller, the problem of switching frequency variation in this nonlinear control method can be easily mitigated [22]. In [23], combination of the SM and backstepping control methods for harmonic compensation of the local loads is proposed in distributed generators. Such an idea can improved the performance and robustness of the closed loop system against model uncertainties, such as grid voltage and frequency, impedance of the coupling inductor, and uncertain load dynamics. However, due to design process of the adaptive backstepping approach, the controlling law will be completely complex and so, its real time calculation can be a time consuming task. As more powerful processors are required for implementation of the combined backstepping-SM controller, it may significantly increase the final cost of the system. Also in [1], adaptive SM approach is employed for closed-loop control of the single phase grid connected photovoltaic system. Current harmonic compensation of the local load as well as maximum power point tracking of the input renewable energy source are main aims of the developed controller. Voltage and parasitic inductance of the grid are estimated with an adaptive estimator. Output current of the inverter is controlled by using a SM and Lyapunov based methods. However, DC link voltage control is performed through a conventional PI controller. Hence,

stability and robustness of the DC link voltage cannot be guaranteed in a wide range of operation.

In Similar problem are also observed in the combination of adaptive control methods with SM [24].

In order to stabilize the non-minimum phase nature of the output current in grid connected voltage source inverters with LCL coupling, a two-loop control in [25] is proposed. The inner loop is used to control the output current of the converter and is designed by using SM method. Also, the reference value of the internal loop is generated in an external loop using a proportional-resonance (PR) controller. In this case, the controller design problem is reduced from a third-order system to a second-order one. However, it is clear that the whole system is not designed based on the SM method and the advantages of the mentioned nonlinear controlling method cannot be obtained in a wide range of system changes.

In recent years, application of the SM controller in other topologies of the grid-connected DC to AC converters, such as impedance source inverters [26] and semi-impedance source inverters [27] is studied. In this case, due to the complexity of the model and the high number of state variables, the extraction of reference values for each of the state variables is associated with complexities. Impedance source converters also have a multi-input-multi-output structure, which adds additional challenges to the controller design. There are similar problems with the application of the SM controlling method in grid-connected multilevel converters, and for this reason, number of articles related to output current control in grid connected multilevel inverters which employ SM approach is limited. The mentioned papers are reviewed below. It is worth noting that due to existence of fundamental differences in the dynamic model of the different multilevel inverters, design process of the SM controller for each of them (clamp diodes, series H-bridges and flying capacitors) is completely different task.

In the reference [28], the SM method is used to control the output current and inject a certain level of active and reactive powers into the grid in multi-level diode clamp inverter. In this paper, a constant voltage source is used in the DC link of the inverter, and for this reason, DC link voltage regulation is not studied. For this reason, if renewable energy sources are used at the DC link, the proposed method in [28] cannot be used to track the maximum power point. It is also necessary to adjust the DC link voltage in FACTS devices and shunt active filters. To do this, in the reference [29] the SM controller is modified with the idea of controlling DC link voltage in diode-clamp multilevel inverters. This is accomplished by introducing an active component in the output current reference value based on the DC link

voltage error by using a linear PI controller. However, in [29] the reference value of the reactive output current is zero, and only the injection of real power from the DC source is studied. It is obvious that the lack of reactive power management in distributed generators will result in high values of the reactive component in distribution network and significantly reduces the grid power factor.

In [30], a hysteresis-band SM controller is used to control the output current in a special 7-level packed U-cell inverter. Less tuning requirement and simplicity of the design are the most important advantages of the closed loop system in [30]. However, stability of the proposed method has not been investigated. Inverter switching frequency changes are also the most important disadvantages of the hysteresis-band SM controllers. To solve this problem in [31], equivalent control is used to design a nonlinear controller in a NPC three level topology. Therefore, it can be directly concluded that such a system is switched according to the PWM pattern and has a fixed frequency. Also in [31], by using the direct Lyapunov theory, stability of the closed-loop system in a wide range of changes in system parameters has been proved. Also, selection of the controlling gains are studied using the linearized model. The controller is able to compensate the reactive and harmonic components of the local load. However, in order to keep voltage of the inverter DC link, an independent current source is employed. So, the controller of [31] is not able to regulate DC link voltage. Moreover, additional modification of the controller for balancing of the DC link capacitors is mandatory.

According to the literature review and research performed by the authors of this article, there is no other report related to output current control in grid connected multi-level inverters.

In this paper, a novel approach for regulation of the output current in the grid-connected three-level flying

capacitor inverter is presented by using the SM method.

In the proposed method, it is possible to control the active and reactive components of the inverter output current independently, and therefore it can be employed for grid connection of the renewable energy resources or for harmonic and reactive power compensation of the local loads.

The designed controller uses an external loop to control the voltage of the inverter DC link and has a constant switching frequency. The stability of the proposed method has also been proved by using the Lyapunov stability theory. The simulation results show that in different operating conditions, the proposed controller has a stable and robust response.

This article is organized as follows. At first the proposed system topology and averaged state space model of the multi-level inverter is discussed. Then, by using the extracted model, the SM controller is designed to control the output current of the grid connected multilevel flying capacitor inverter. Finally, developed controller is investigated by PC based simulations in the MATLAB/SIMULINK software.

System Modeling

Circuit topology of the grid connected flying capacitor multilevel inverter is shown in Fig. 1. Also, phase-shifted pulse width modulation (PWM) switching of the phase-A is illustrated in Fig. 2. Similar waveforms can be introduced for phase B and C due to symmetrical operation of the different phases. In this figure, u_a is amplitude modulation index and control effort of the phase A. Duty cycles of the S_{1a} and S_{2a} can be calculated considering the similarity of the following triangles.

$$\Delta ABC \sim DBE : D_1 = \frac{T_{on1}}{T} = \frac{u_a + 1}{2} \tag{1}$$

$$\Delta ABC \sim AED : D_2 = \frac{T_{on2}}{T} = \frac{u_a - 1}{2} \tag{2}$$

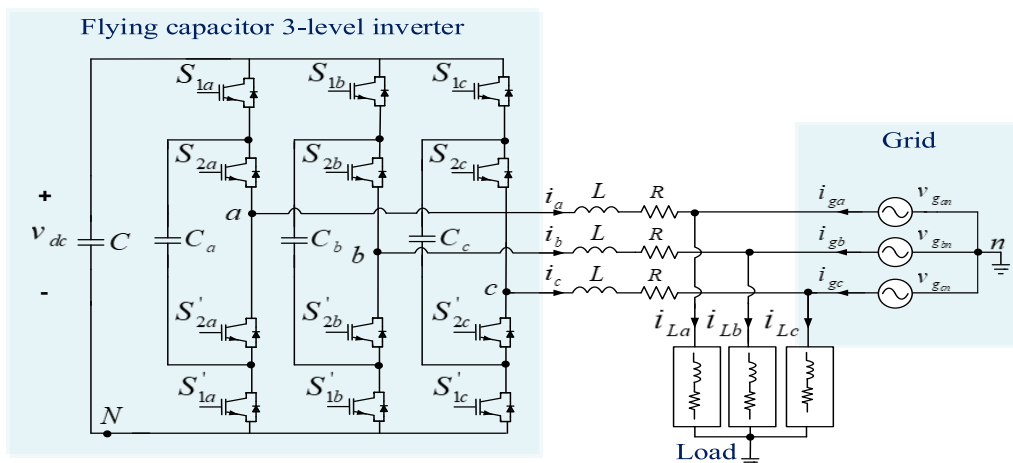
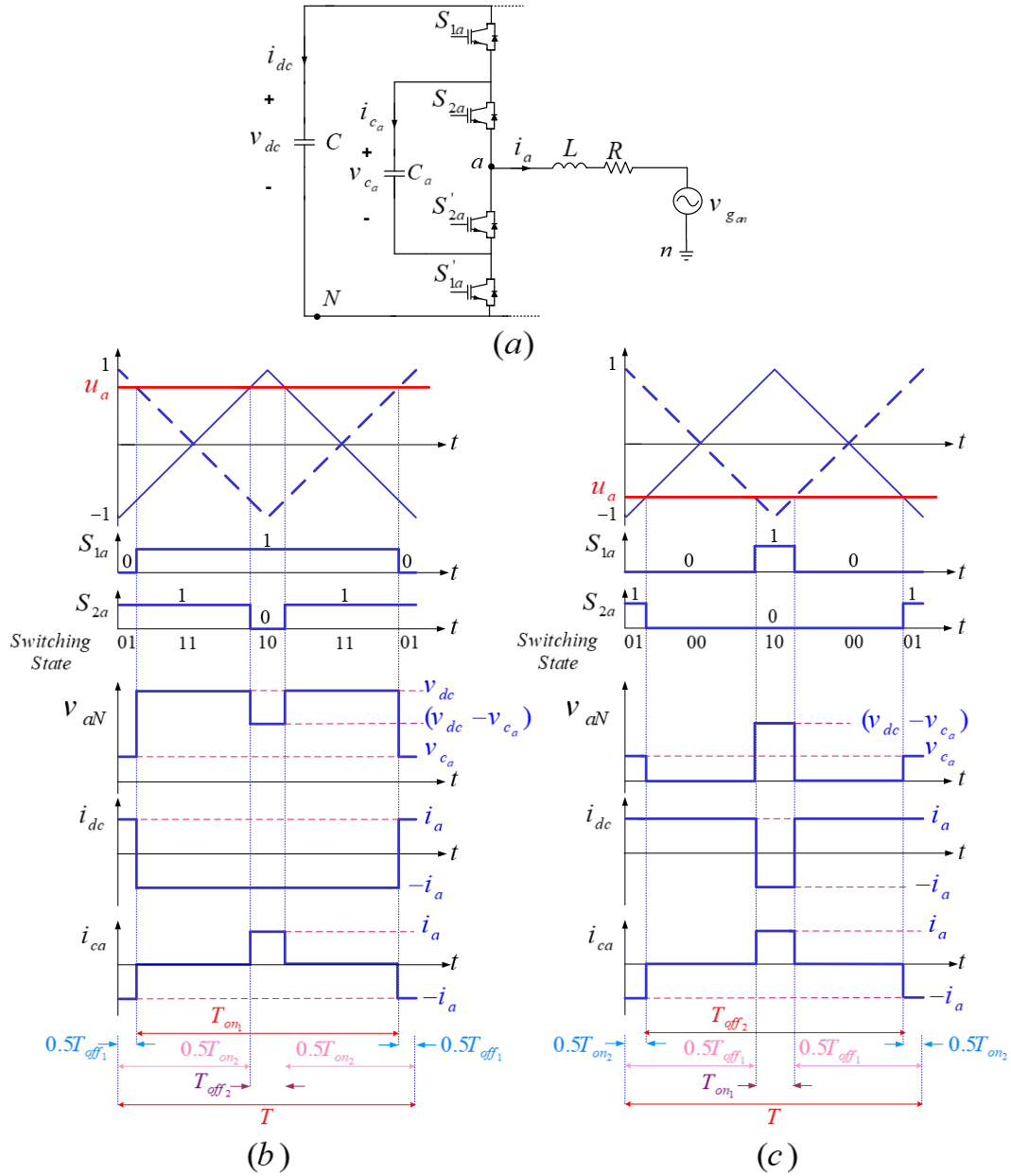


Fig. 1: Topology of the grid connected multi-level inverter.


 Fig. 2: Phase shifted PWM switching of the first leg (a) for positive (b) and negative (c) control efforts (u_a).

Clearly as u_a is amplitude modulation index of the inverter, so operation of the system can be divided into two different modes. When $u_a > 0$:

$$\begin{aligned} \bar{v}_{aN} &= \frac{1}{T} (v_{ca} T_{off1} + v_{dc} T_{on1} - v_{ca} T_{off2}) \\ &= \frac{v_{dc}}{2} (u_a + 1) \end{aligned} \quad (3)$$

and for $u_a < 0$:

$$\begin{aligned} \bar{v}_{aN} &= v_{ca} (T_{on2}) + (v_{dc} - v_{ca}) \frac{T_{on1}}{T} \\ &= \frac{v_{dc}}{2} (u_a + 1) \end{aligned} \quad (4)$$

So, line voltages of the three-phase system can be written as:

$$\begin{cases} \bar{v}_{aN} = \frac{v_{dc}}{2} (u_a + 1) \\ \bar{v}_{bN} = \frac{v_{dc}}{2} (u_b + 1) \\ \bar{v}_{cN} = \frac{v_{dc}}{2} (u_c + 1) \end{cases}; \begin{cases} \bar{v}_{ab} = \frac{v_{dc}}{2} (u_a - u_b) \\ \bar{v}_{bc} = \frac{v_{dc}}{2} (u_b - u_c) \\ \bar{v}_{ca} = \frac{v_{dc}}{2} (u_c - u_a) \end{cases} \quad (5)$$

Equivalent model of the three phase system is illustrated in Fig. 3 where n' is virtual ground of the inverter DC link. So, average values of the three phase voltages can be related to its corresponding modulation index as:

$$\begin{cases} \bar{v}_{an'} = \frac{v_{dc}}{2} u_a \\ \bar{v}_{bn'} = \frac{v_{dc}}{2} u_b \\ \bar{v}_{cn'} = \frac{v_{dc}}{2} u_c \end{cases} \quad (6)$$

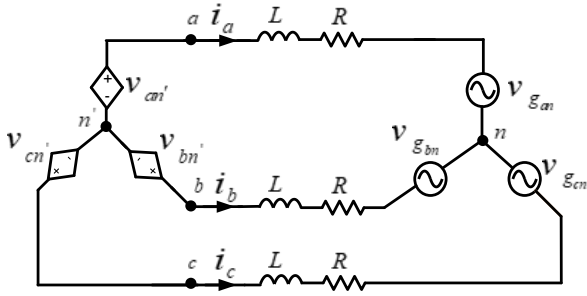


Fig. 3: Equivalent model of the grid connected inverter.

So, equivalent model of the grid connected inverter can be summarized according to Fig. 4.

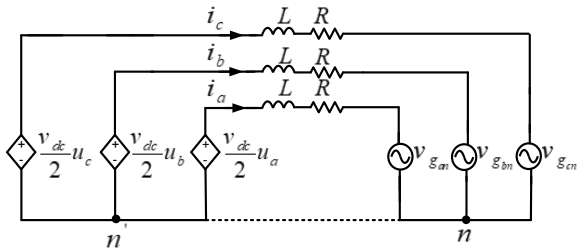


Fig. 4: Summarized equivalent model of the system.

In a balanced three phase systems, n and n' have a same potential. So:

$$\frac{di_a}{dt} = \frac{1}{L} (v_{an'} - v_{gan} - Ri_a) \quad (7)$$

$$\frac{di_b}{dt} = \frac{1}{L} (v_{bn'} - v_{gbn} - Ri_b) \quad (8)$$

$$\frac{di_c}{dt} = \frac{1}{L} (v_{cn'} - v_{gcn} - Ri_c) \quad (9)$$

With regard to current of the DC link capacitor and considering i_a , while $u_a > 0$, i_a the following equation can be written:

$$\begin{aligned} i_{dc} &= \frac{1}{T} i_a (T_{off1} - T_{on1}) = i_a (1 - 2D_1) \\ &= i_a \left(1 - 2 \left(\frac{u_a + 1}{2} \right) \right) \\ &= -i_a u_a \end{aligned} \quad (10)$$

So considering the three phase system, current of the DC link capacitor will be modeled as:

$$i_{dc} = -(i_a u_a + i_b u_b + i_c u_c) = C \frac{dv_{dc}}{dt} \quad (11)$$

and while $u_a < 0$:

$$i_{dc} = i_a \left(\frac{T_{off1} - T_{on1}}{T} \right) = -i_a u_a \quad (12)$$

Also, current of the C_a can be summarized in different operating modes as:

$$u_a > 0 : i_{ca} = \frac{1}{T} i_a (-T_{off1} + T_{on1}) = 0 \quad (13)$$

$$u_a < 0 : i_{ca} = \frac{1}{T} i_a (-T_{on2} + T_{on1}) = 0 \quad (14)$$

So, if $T_{on1} = T_{on2}$ and $T_{off1} = T_{off2}$, average value of the i_{ca} will be zero and voltage of the C_a will not change in steady-state and dynamic operational conditions of the converter. As a result, voltages of the flying capacitors are not an independent state variables and hence the multilevel grid connected inverter in Fig.1 has 4 state variable which are currents of the coupling inductors as well as voltage of the DC link capacitor. Briefly, the following equations can be considered for dynamics of the flying capacitors in phase shifted PWM switching strategy:

$$\frac{dv_{ca}}{dt} = 0 ; \frac{dv_{cb}}{dt} = 0 ; \frac{dv_{cc}}{dt} = 0 \quad (15)$$

So considering equations (6)-(9) and (11), averaged state space model of the system can be written as follows:

$$\begin{bmatrix} \frac{di_a}{dt} \\ \frac{di_b}{dt} \\ \frac{di_c}{dt} \\ \frac{dv_{dc}}{dt} \end{bmatrix} = \begin{bmatrix} -\frac{R}{L} & 0 & 0 & \frac{u_a}{2L} \\ 0 & -\frac{R}{L} & 0 & \frac{u_b}{2L} \\ 0 & 0 & -\frac{R}{L} & \frac{u_c}{2L} \\ -\frac{u_a}{C} & -\frac{u_b}{C} & -\frac{u_c}{C} & 0 \end{bmatrix} \begin{bmatrix} i_a \\ i_b \\ i_c \\ v_{dc} \end{bmatrix} + \begin{bmatrix} -\frac{1}{L} v_{gan} \\ -\frac{1}{L} v_{gbn} \\ -\frac{1}{L} v_{gcn} \\ 0 \end{bmatrix} \quad (16)$$

Sliding Mode Controller Design

Averaged state space model of the converter is given in (16). In this section, an SM controller is developed for output current control of the multilevel grid connected inverter. As dynamics of the DC link capacitor voltage is completely slow compared to output currents of the converter, so during the SM controller design, changes of the DC link capacitor voltage can be neglected for simplicity of the developed closed loop system. So, model of the converter $dq0$ frame can be rewritten as follows:

$$\begin{aligned} \frac{d}{dt} \begin{bmatrix} i_q \\ i_d \\ i_0 \end{bmatrix} &= \begin{bmatrix} -\frac{R}{L} & -\omega & 0 \\ \omega & -\frac{R}{L} & 0 \\ 0 & 0 & -\frac{R}{L} \end{bmatrix} \begin{bmatrix} i_q \\ i_d \\ i_0 \end{bmatrix} \\ &+ \begin{bmatrix} -\frac{1}{L} & 0 & 0 \\ 0 & -\frac{1}{L} & 0 \\ 0 & 0 & -\frac{1}{L} \end{bmatrix} \begin{bmatrix} v_{gq} \\ v_{gd} \\ v_{g0} \end{bmatrix} \\ &+ \begin{bmatrix} \frac{V_{dc}}{2L} & 0 & 0 \\ 0 & \frac{V_{dc}}{2L} & 0 \\ 0 & 0 & \frac{V_{dc}}{2L} \end{bmatrix} \begin{bmatrix} u_q \\ u_d \\ u_0 \end{bmatrix} \end{aligned} \quad (17)$$

It should be noted that $f^{abc} = [T_{qd0}(\theta)]^{-1} f^{qd0}$ is employed for transformation between abc and dq0 frames -where:

$$T^{-1}(\theta) = \begin{bmatrix} \cos(\theta) & \sin(\theta) & 1 \\ \cos(\theta - \frac{2\pi}{3}) & \sin(\theta - \frac{2\pi}{3}) & 1 \\ \cos(\theta + \frac{2\pi}{3}) & \sin(\theta + \frac{2\pi}{3}) & 1 \end{bmatrix} \quad (18)$$

In (17), $X(t) = [i_q \ i_d \ i_0]^T$ is state vector of the dynamic model. In this case, u_q , u_d and u_0 are controlling inputs of the system. Also, state variables of the model are control outputs.

According to (17), distributed model of the grid connected multilevel inverter can be rewritten as follows:

$$\dot{x}_1 = \left(-\frac{R}{L}x_1 - \omega x_2 - \frac{1}{L}v_{gq}\right) + \left(\frac{V_{dc}}{2L}u_q\right) \quad (19)$$

$$\dot{x}_2 = \left(\omega x_1 - \frac{R}{L}x_2 - \frac{1}{L}v_{gd}\right) + \left(\frac{V_{dc}}{2L}u_d\right) \quad (20)$$

$$\dot{x}_3 = \left(-\frac{R}{L}x_3 - \frac{1}{L}v_{g0}\right) + \left(\frac{V_{dc}}{2L}u_0\right) \quad (21)$$

In the general form, system dynamics can be described as:

$$\begin{aligned} \dot{x}_1 &= f_1(x_1, x_2, x_3, t) + b_1(x_1, x_2, x_3, t)u_q \\ &= (\bar{f}_1 + \tilde{f}_1) + (\bar{b}_1 + \tilde{b}_1)u_q \end{aligned} \quad (22)$$

$$\begin{aligned} \dot{x}_2 &= f_2(x_1, x_2, x_3, t) + b_2(x_1, x_2, x_3, t)u_d \\ &= (\bar{f}_2 + \tilde{f}_2) + (\bar{b}_2 + \tilde{b}_2)u_d \end{aligned} \quad (23)$$

$$\begin{aligned} \dot{x}_3 &= f_3(x_1, x_2, x_3, t) + b_3(x_1, x_2, x_3, t)u_0 \\ &= (\bar{f}_3 + \tilde{f}_3) + (\bar{b}_3 + \tilde{b}_3)u_0 \end{aligned} \quad (24)$$

where \bar{f} and \bar{b} are nominal values of the model parameters. Also, \tilde{f} and \tilde{b} are uncertainty of f and b respectively. In order to control output current of the inverter in d and q axes, two sliding surface can be defined as follows:

$$\begin{aligned} S &= \alpha[X_{ref} - X] + \beta X_{int} = \begin{bmatrix} S_1 \\ S_2 \end{bmatrix} \\ &= \begin{bmatrix} \alpha_1 & 0 \\ 0 & \alpha_2 \end{bmatrix} \begin{bmatrix} (x_1^* - x_1) \\ (x_2^* - x_2) \end{bmatrix} \\ &+ \begin{bmatrix} \beta_1 & 0 \\ 0 & \beta_2 \end{bmatrix} \begin{bmatrix} \int (x_1^* - x_1) dt \\ \int (x_2^* - x_2) dt \end{bmatrix} \end{aligned} \quad (25)$$

where x_1^* and x_2^* are references of the state variables x_1 and x_2 . As it is seen in (25), integrals of the current errors are added to sliding surfaces to cancel the steady state error of the response. In this equation, α and β are

positive design parameters.

In order to present SM controller design in a general form, state space model of the converter can be rewritten in a compact form as follows:

$$\begin{aligned} \dot{X} &= \begin{bmatrix} \dot{x}_1 \\ \dot{x}_2 \end{bmatrix} = \underbrace{(\bar{F} + \tilde{F})}_F + \underbrace{(\bar{B} + \tilde{B})}_B U \\ &= \begin{bmatrix} f_1 \\ f_2 \end{bmatrix} + \begin{bmatrix} b_1 & 0 \\ 0 & b_2 \end{bmatrix} \begin{bmatrix} u_q \\ u_d \end{bmatrix} \end{aligned} \quad (26)$$

The proposed SM controller includes equivalent (\bar{u}_q, \bar{u}_d) and nonlinear (\tilde{u}_q, \tilde{u}_d) components as:

$$U = \bar{U} + \tilde{U} = \begin{bmatrix} u_q \\ u_d \end{bmatrix} = \begin{bmatrix} \bar{u}_q + \tilde{u}_q \\ \bar{u}_d + \tilde{u}_d \end{bmatrix} \quad (27)$$

Nonlinear component of the SM controller is responsible for improvement of the robustness and stability of the system against changes of the uncertain parameters. These components can be assumed as follows:

$$\tilde{u}_q = k_1 \text{sgn}(S_q) \quad (28)$$

$$\tilde{u}_d = k_2 \text{sgn}(S_d) \quad (29)$$

Equivalent SM controllers can be obtained by setting derivative of the sliding surface into zero in (25) as:

$$\dot{S} = \alpha(\dot{X}_{ref} - \dot{X}) + \beta \dot{X}_{int} = 0 \quad (30)$$

By substituting (26) in (30), equivalent SM controller can be obtained in the general form as:

$$\bar{U} = (\bar{B})^{-1}(\dot{X}_{ref} - \bar{F} + \alpha^{-1}\beta\dot{X}_{int}) \quad (31)$$

$$\begin{aligned} \bar{u}_q &= \frac{2\left(\alpha_1 v_{gq} + \alpha_1 L \frac{dx_1^*}{dt} - \beta_1 L x_1 + \beta_1 L x_1^* + \alpha_1 R x_1 + \alpha_1 L \omega x_2\right)}{\alpha_1 v_{dc}} \end{aligned} \quad (32)$$

$$\begin{aligned} \bar{u}_d &= \frac{2\left(\alpha_2 v_{gd} + \alpha_2 L \frac{dx_2^*}{dt} - \beta_2 L x_2 + \beta_2 L x_2^* + \alpha_2 R x_2 - \alpha_2 L \omega x_1\right)}{\alpha_2 v_{dc}} \end{aligned} \quad (33)$$

Finally, according to averaged state space model of the converter, equivalent sliding mode controller in (31) can be summarized for three level grid-connected flying capacitor as (32) and (33).

As it has been described previously, to improve robustness of the proposed controller against changes of the uncertain parameters, developed equivalent SM controller in (31) is combined with a nonlinear component.

$$\bar{U} = (\bar{B})^{-1}(\dot{X}_{ref} - \bar{F} + \alpha^{-1}\beta\dot{X}_{int} + K \text{sgn}(S)) \quad (34)$$

where the parameter K is

$$K = \begin{bmatrix} k_1 & \mathbf{0} \\ \mathbf{0} & k_2 \end{bmatrix} \quad (35)$$

The extracted SM controller in (34) has two parts. First one is equivalent SM and second component $[Ksgn(S)]$ is used for improving stability and robustness of the closed-loop system. It should be noted that the equivalent controllers of the system are given in (32) and (33).

Based on (30) and (34):

$$\begin{aligned} \dot{S} = \alpha \dot{X}_{ref} - \alpha(F + B(\bar{B})^{-1}(\dot{X}_{ref} - \bar{F} \\ + \alpha^{-1}\beta \dot{X}_{int} + Ksgn(S))) \\ + \beta \dot{X}_{int} \end{aligned} \quad (36)$$

In order to investigate stability of the developed controller, the input matrix, B can be introduced as

$$B = \bar{B} + \tilde{B} = (I + \Delta)\bar{B} \quad |\Delta_{ij}| \leq D_{ij} \quad i, j = 1, 2 \quad (37)$$

where $I_{2 \times 2}$ is an identity matrix. So, it is clear that $B(\bar{B})^{-1} = (I + \Delta)$. Also, elements of the $\Delta_{2 \times 2}$ are defined as Δ_{ij} .

According to (26), it can be concluded that $\Delta_{12} = \Delta_{21} = 0$. So, \dot{S} in (36) can be simplified as

$$\begin{aligned} \dot{S} = -\alpha\Delta\alpha^{-1}\beta\dot{X}_{int} + \alpha(\bar{F} - F) \\ - \alpha(\Delta + I)Ksgn(S) \\ - \alpha\Delta\dot{X}_{ref} + \alpha\Delta\bar{F} \end{aligned} \quad (38)$$

To evaluate stability and robustness of the proposed controller, the following criteria should be considered

$$S_i \dot{S}_i \leq -\mu_i |S_i| \quad (\mu_i > 0) \quad (39)$$

where μ_i is the design constant. Considering (38), (39) can be simplified as follows for S_1

$$\begin{aligned} S_1(\alpha_1(\bar{f}_1 - f_1) - \alpha_1 k_1(1 + \Delta_{11})sgn(S_1) \\ - \beta_1 \Delta_{11}(x_1^* - x_1) \\ + \alpha_1 \Delta_{11}(\bar{f}_1 - \dot{x}_1^*)) \\ \leq |S_1|(\alpha_1 |\bar{f}_1 - f_1| \\ - \alpha_1 k_1(1 - D_{11}) \\ - \beta_1 D_{11}|x_1^* - x_1| \\ + \alpha_1 D_{11}|\bar{f}_1 - \dot{x}_1^*|) \\ \leq -\mu_1 |S_1| \end{aligned} \quad (40)$$

Since $|f_i - \hat{f}_i| \leq f_{i,max}$, (40) can be reduced to

$$\alpha_1 f_{1,max} - \beta_1 D_{11}|x_1^* - x_1| + \alpha_1 D_{11}|\bar{f}_1 - \dot{x}_1^*| \\ + \mu_1 \leq \alpha_1 k_1(1 - D_{11}) \quad (41)$$

Similarly, (39) can be written as follows for S_2

$$\alpha_2 f_{2,max} - \beta_2 D_{22}|x_2^* - x_2| + \alpha_2 D_{22}|\bar{f}_2 - \dot{x}_2^*| \\ + \mu_2 \leq \alpha_2 k_2(1 - D_{22}) \quad (42)$$

Considering (41) and (42), in order to guarantee the stability of the developed SM controller, the control

gains should be selected according to the following conditions

$$k_1 \geq (1 - D_{11})^{-1}(f_{1,max} \\ - \alpha_1^{-1}\beta_1 D_{11}|x_1^* - x_1| \\ + D_{11}|\bar{f}_1 - \dot{x}_1^*| + \alpha_1^{-1}\mu_1) \quad (43)$$

$$k_2 \geq (1 - D_{22})^{-1}(f_{2,max} \\ - \alpha_2^{-1}\beta_2 D_{22}|x_2^* - x_2| \\ + D_{22}|\bar{f}_2 - \dot{x}_2^*| + \alpha_2^{-1}\mu_2) \quad (44)$$

The final SM control law can be obtained by adding of the nonlinear component into equivalent terms in (32) and (33). Its block diagram is illustrated for u_q in Fig. 5. Also, in order to adjust voltages of the flying capacitor, final modulation indexes of the multilevel inverter should be modified. In fact, small changes should be applied according to flying capacitor voltage error and sign of the output current. This idea is shown for lag A in Fig. 6 where u_{a1} and u_{a2} are amplitude modulation indexes for switches S_{a1} and S_{a2} respectively.

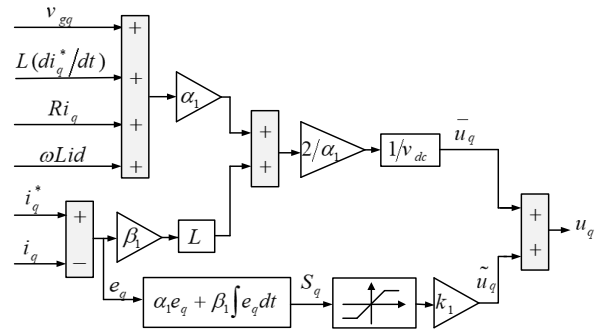


Fig. 5: Implementation of the proposed SM controller for u_q .

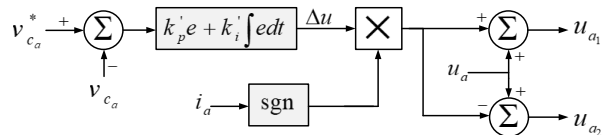


Fig. 6: Modification of the amplitude modulation index for regulation of the flying capacitors voltage (phase A).

Finally, block diagram of the proposed controller is shown in Fig. 7. The current controller is calculated based on reference currents and grid voltage in dq frame. Active reference current (i_d^*) is defined based on DC link voltage error through a linear PI controller. In shunt compensators, there is no independent voltage source on DC link and hence, DC link capacitor voltage is regulated by absorbing an active power from the grid which is equal to inverter power loss in shunt compensators. Also, inactive reference current (i_q^*) is calculated based on local load requirement. For example in shunt active power filters, i_q^* is equal to inactive component of the load current.

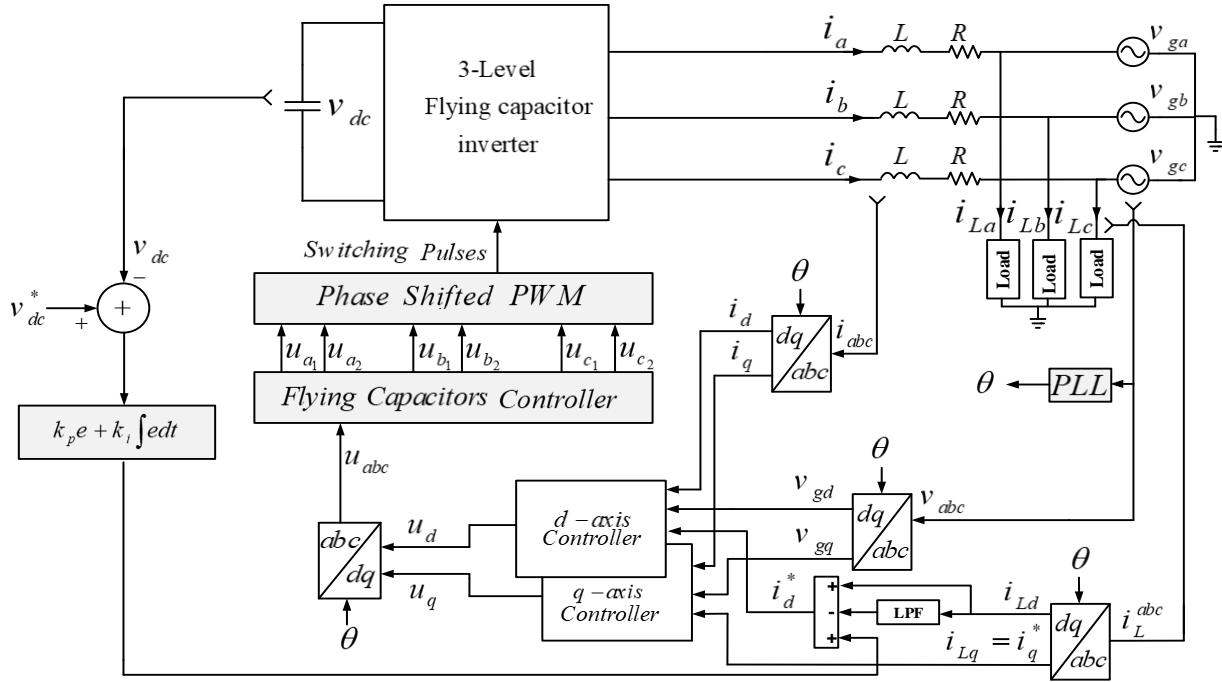


Fig. 7: Block diagram of the proposed SM controller for grid connected multilevel flying capacitor inverter

Simulation Results

In order to verify response of the proposed current controller in Fig. 7, grid connected three level flying capacitor inverter is simulated in MATLAB/Simulink software.

Nominal values of the system parameters as well as controller gains are listed in Table 1 and Table 2.

To investigate the steady-state and dynamic responses of the proposed closed loop system in reactive power compensating mode, the 20kVA resistive-inductive (RL) branch with 0.6 power factor is employed as a main local load. Also, active power filtering capability of the system is studied in the next tests.

Table 1: Nominal values of the system parameters

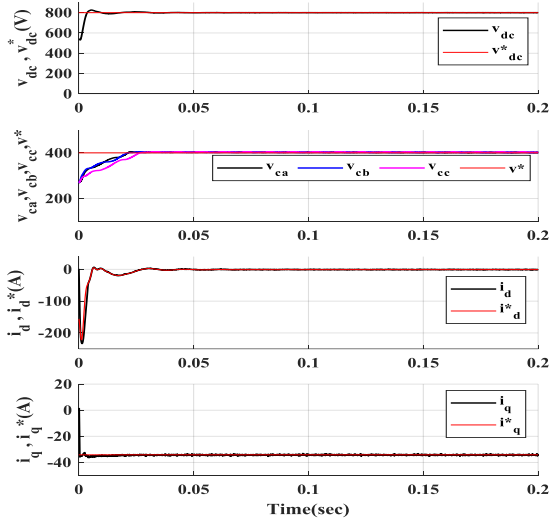
Parameter	Symbol	Value
Grid voltage(rms)	v_g	220V
Grid frequency	f	50Hz
Switching frequency	f_s	20kHz
DC-Link and flying capacitors	C, C_a, C_b and C_c	1200 μ f
DC-side capacitor reference voltage	v_{dc}^*	800V
AC-side coupling inductor	L	1mH
AC-side coupling resistor	R	0.1 Ω

Table 2: Controller gains

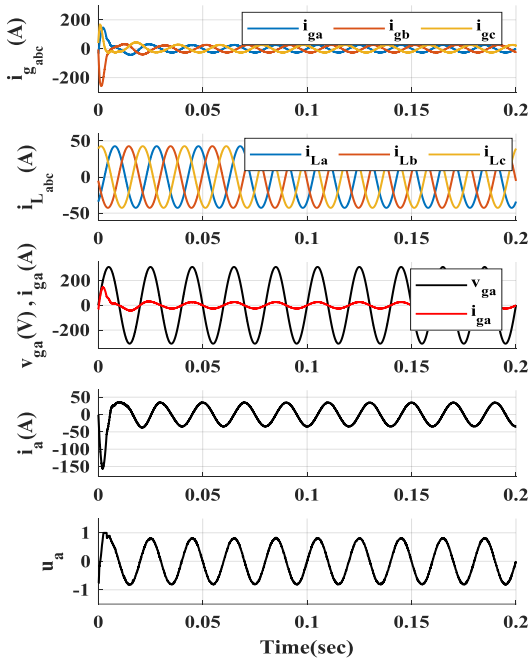
Parameter	Value
k_p	0.8
k_i	15
α_1, α_2	20
β_1, β_2	100
k_1, k_2	1
k'_p	0.05
k'_i	0.1

A. Test 1

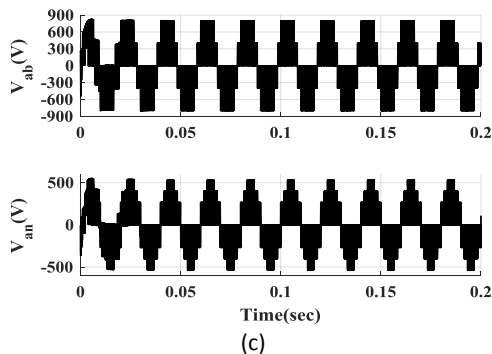
In this test, considering nominal value of the RL local load, response of the designed controller is investigated during system startup. Reference values of the DC link and flying capacitors are 800 V and 400 V respectively. Reactive reference current (i_q) of the closed loop system is defined according to local load reactive component. Also considering power loss of the inverter, the active current reference (i_d) is generated in the outer loop to stabilize the capacitor voltages on their desired values. According to Fig. 8a, Fig. 8b and Fig. 8c, it is seen that the proposed controller is able to stabilize the reactive power compensator satisfactorily. Also, during the steady-state conditions, steady-state error of the system state variables is zero. Due to reactive power compensation through the grid connected inverter, grid voltage and current are in phase after the transient interval of the response.



(a)



(b)



(c)

Fig. 8: Response of the system during startup and steady-state conditions; (a) State variables and reference values, (b) Grid currents and voltages, (c) Phase and line voltages of the inverter.

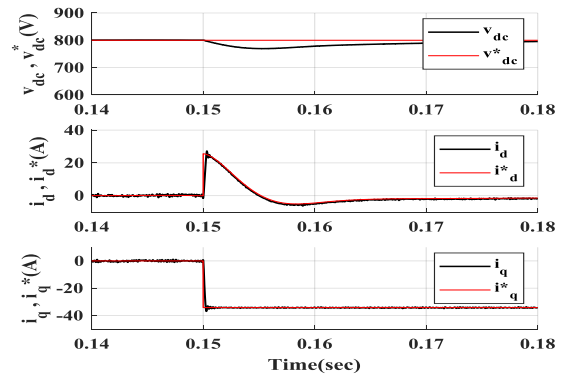
B. Test 2

In Fig. 9, dynamic response of the inner current controller is evaluated. At first, it is assumed that outer

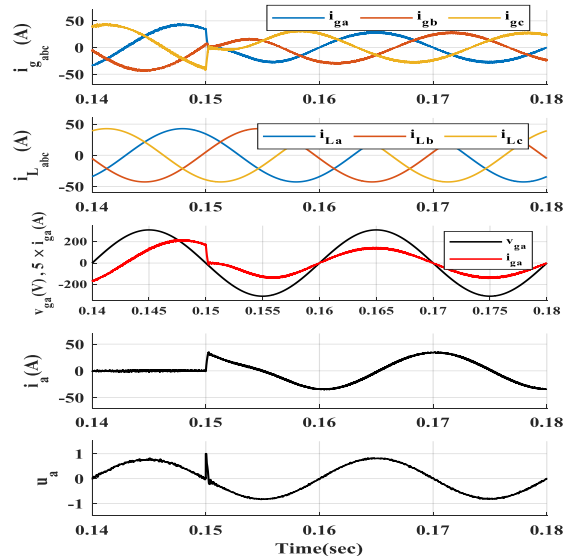
controller regulates the DC link voltage without reactive compensation. Then, in $t=0.15s$ internal current loop is activated to compensate the nominal RL local load. It is seen that the proposed SM controller has fast dynamic response and is able to stabilize the output current of the grid-connected multilevel inverter with zero steady state error.

C. Test 3

In Fig. 10, dynamic response of the DC link and flying capacitor voltages are studied. At first, the closed loop system starts to compensate the nominal local load. Then, DC link voltage reference is stepped up from 750 V to 950 V. Also, references of the flying capacitor voltages are increased from 375 V to 475 V. In spite of changes of the reference voltage in a wide range, it is seen that the outer loop is stabilizing the DC link voltage with fast dynamics. Moreover, the overshoot of the response is completely acceptable which guarantees safe operation of the electrolyte type capacitors on the inverter's DC link. Furthermore, outer voltage loop has no steady state error due to employment of the integral term in the final controlling law of the controller.



(a)



(b)

Fig. 9: Transient response of the internal SM current controller; (a) State variables and reference values, (b) Grid currents and voltages.

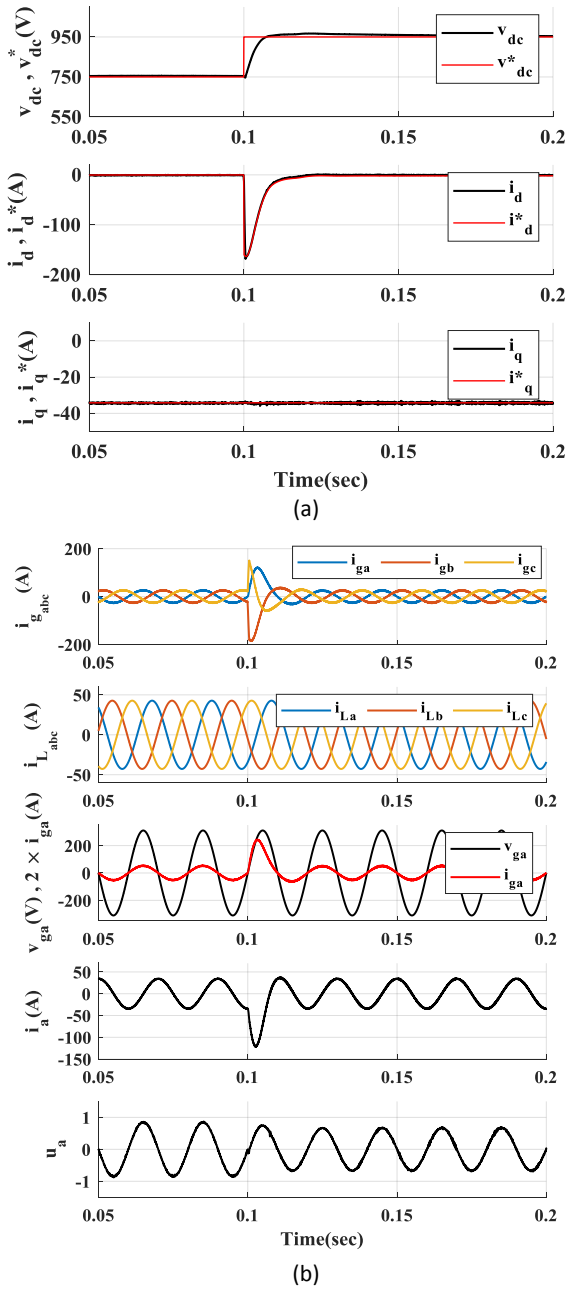


Fig. 10: Transient response of outer voltage controller during step changes of the DC link voltage references; (a) State variables and reference values, (b) Grid currents and voltages.

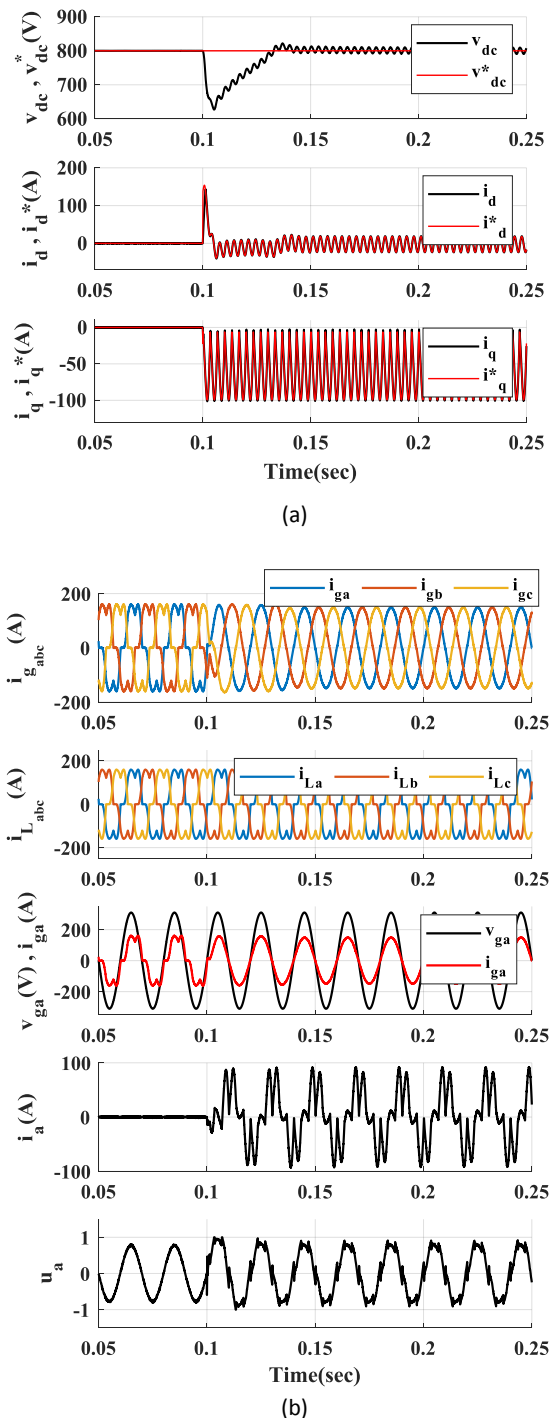
D. Test 4

In Fig. 11, dynamic response of the proposed controller during active power filtering mode is illustrated. At first, system is started to regulate the DC link capacitors. In this condition, reference of the i_q is zero and inverter output power is equal to its power loss to keep the DC link capacitors regulated. Then, in $t=0.1s$, the internal SM control system is activated to compensates the local load.

So, the grid current is non-sinusoidal before compensation as it includes harmonic components of

the nonlinear load. It is seen that after startup of the internal current loop, grid current will be pure sinusoidal with acceptable THD value. It should be noted that THD of the grid current is 20.61% before compensation that is reduced to 1.34% after activation of the internal loop of the proposed control approach.

So, proposed control strategy can be employed in active power filtering mode as well. It is seen that, in spite of fast changes of the inverter reference current, the proposed control strategy can track the reference value accurately.



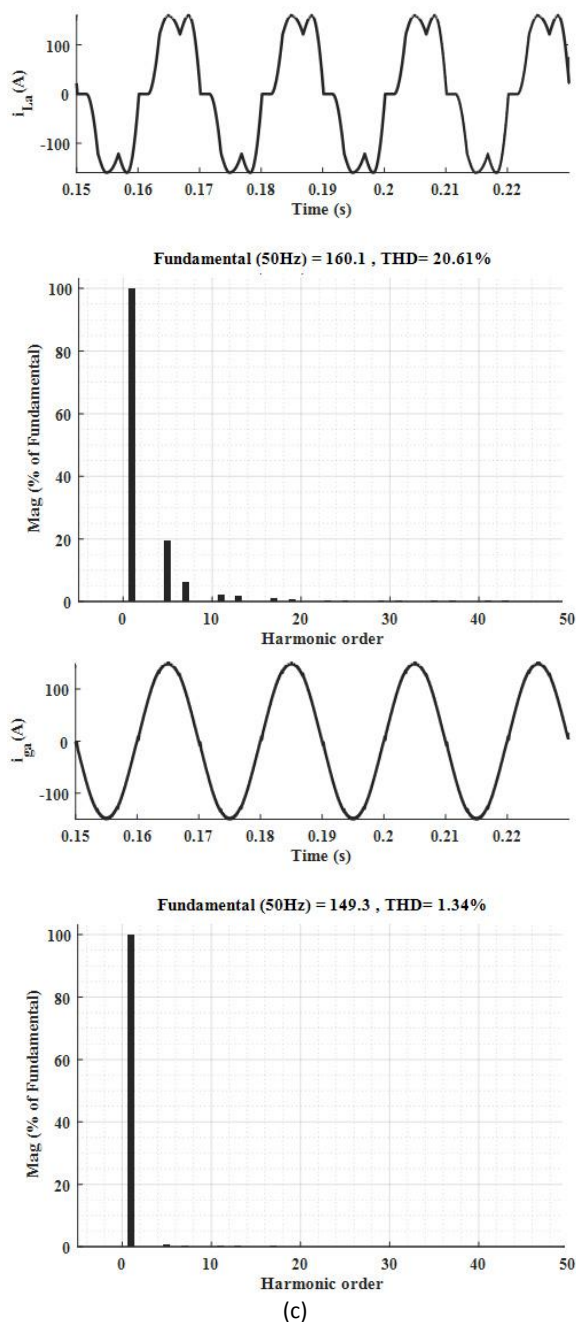


Fig. 11: Dynamic response of the proposed controller during active power filtering mode; (a) State variables and reference values, (b) Grid currents and voltages, (c) THD of the load and grid currents for phase A.

Conclusion

In this paper, a general purpose sliding mode controller is proposed for output current control of the grid connected multi-level flying capacitor inverter. The proposed controller enjoys very fast dynamic response, so it can be employed in wide ranges of application e.g. reactive compensation and harmonic mitigation modes. In active power filtering operation, it is able to eliminate harmonic components of the grid from 20.61% to 1.34% which is compatible with IEEE and IEC standards. The

designed controller uses an external loop to control the voltage of the inverter DC link and has a constant switching frequency. The stability of the proposed method has also been proved by using the Lyapunov stability theory. The simulation results show that in different operating conditions, the proposed controller has a stable and robust response.

Author Contributions

This paper is related to M.Sc. thesis of Miss Negin Ghaffari. All of the authors have the same contribution in different parts of the paper including system modeling, controller design and simulation.

Acknowledgment

The author gratefully acknowledges the Power Quality Lab of Arak University of Technology.

Conflict of Interest

The author declares that there is no conflict of interests regarding the publication of this manuscript. In addition, the ethical issues, including plagiarism, informed consent, misconduct, data fabrication and/or falsification, double publication and/or submission, and redundancy have been completely observed by the authors.

Abbreviations

<i>SM</i>	Sliding Mode
<i>PWM</i>	Pulse Width Modulation
<i>PI</i>	Proportional Integral
<i>THD</i>	Total Harmonic Distortion
<i>FACTS</i>	Flexible AC Transmission Systems
<i>NPC</i>	Neutral Point Clamped

References

- [1] Z. Hekss, A. Abouloifa, I. Lachkar, F. Giri, S. Echalih, J.M. Guerrero, "Nonlinear adaptive control design with average performance analysis for photovoltaic system based on half bridge shunt active power filter," *Int. J. Electr. Power Energy Syst.*, 125, 2021.
- [2] Q. Su, W. Quan, W. Quan, G. Cai, J. Li, "Improved robust adaptive backstepping control approach on STATCOM for non-linear power systems," *IET Gener. Transm. Distrib.*, 11(3): 3428-3437, 2017.
- [3] M. Salimi, J. Soltani, A. Zaki pour, "Experimental design of the adaptive backstepping control technique for single-phase shunt active power filters," *IET Power Electron.*, 10(8): 911-918, 2017.
- [4] A. Zaki pour, S.S. Kojori, M. Salimi, "Low-Cost wind power conversion system based on permanent magnet synchronous generator and grid connected single-phase impedance source inverter," in *Proc. 2019 International Power System Conference (PSC): 616-622, 2019.*
- [5] M.A. Hannan, P.J. Ker, M.S.H. Lipu, Z.H. Choi, M.S.A. Rahman, K.M. Muttaqi, et al., "State of the art of solid-state transformers: Advanced topologies, implementation issues, recent progress and improvements," *IEEE Access*, 8: 19113-19132, 2020.
- [6] X. Li, Y. Tan, X. Liu, Q. Liao, B. Sun, G. Cao, et al., "A cost-benefit analysis of V2G electric vehicles supporting peak shaving in Shanghai," *Electr. Power Syst. Res.*, 179: 106058, 2020.

- [7] Y.P. Siwakoti, P. Fang Zheng, F. Blaabjerg, L. Poh Chiang, G.E. Town, "Impedance-Source Networks for Electric Power conversion Part I: A topological review," *IEEE Trans. Power Electron.*, 30(2): 699-716, 2015.
- [8] P. Hamedani, A. Shoulai, "Utilization of CHB multilevel inverter for harmonic reduction in fuzzy logic controlled multiphase LIM drives," *J. Electr. Comput. Eng. Innovations (JECEI)*, 8(1): 19-30, 2019.
- [9] M.T. Bina, D.C. Hamill, "Average circuit model for angle-controlled STATCOM," *IEE J. Electr. Power Appl.*, 152(3): 653-659, 2005.
- [10] X. Zhao, L. Chang, "Active and reactive power decoupling control of grid-connected inverters in stationary reference frame," *Chin. J. Electr. Eng.*, 3(3): 18-24, 2017.
- [11] M. Cespedes, J. Sun, "Adaptive control of grid-connected inverters based on online grid impedance measurements," *IEEE Trans. Sustainable Energy*, 5(2): 516-523, 2014.
- [12] Y. Wang, B. Ren, Q.-C. Zhong, "Robust power flow control of grid-connected inverters," *IEEE Trans. Ind. Electron.*, 63(11): 6887-6897, 2016.
- [13] A. Akhavan, H.R. Mohammadi, J.C. Vasquez, J. M. Guerrero, "Passivity-based design of plug-and-play current-controlled grid-connected inverters," *IEEE Trans. Power Electron.*, 35(2): 2135-2150, 2019.
- [14] H. Makhamreh, M. Sleiman, O. Kükrer, K. Al-Haddad, "Lyapunov-based model predictive control of a PUC7 grid-connected multilevel inverter," *IEEE Trans. Ind. Electron.*, 66(9): 7012-7021, 2018.
- [15] M. Salimi, J. Soltani, A. Zakipour, N.R. Abjadi, "Hyper-plane sliding mode control of the DC-DC buck/boost converter in continuous and discontinuous conduction modes of operation," *IET Power Electron.*, 8(8): 1473-1482, 2015.
- [16] J.-J.E. Slotine, W. Li, *Applied nonlinear control* vol. 199: Prentice hall Englewood Cliffs, NJ, 1991.
- [17] S. Mohammadi, H. Mosaddegh, M. Yousefian, "Mitigation of switching harmonics in shunt active power filter based on variable structure control approach," *J. Electr. Comput. Eng. Innovations (JECEI)*, 1(2): 83-88, 2013.
- [18] H. Zahedi, G. Arab Markadeh, S. Taghipour, "Real-time implementation of sliding mode control for cascaded doubly fed induction generator in both islanded and grid connected modes," *J. Electr. Comput. Eng. Innovations (JECEI)*, 8(2): 285-296, 2020.
- [19] H. Xiang, Y. Xu, L. Tao, H. Lang, C. Wenjie, "A Sliding-Mode controller with multiresonant sliding surface for single-phase grid-connected VSI with an LCL Filter," *IEEE Trans. Power Electron.*, 28(5): 2259-2268, 2013.
- [20] S.-W. Kang, K.-H. Kim, "Sliding mode harmonic compensation strategy for power quality improvement of a grid-connected inverter under distorted grid condition," *IET Power Electron.*, 8(8): 1461-1472, 2015.
- [21] H. Komurcugil, S. Ozdemir, I. Sefa, N. Altin, O. Kukrer, "Sliding-mode control for single-phase grid-connected LCL-Filtered VSI with double-band hysteresis scheme," *IEEE Trans. Ind. Electron.*, 63(2): 864-873, 2016.
- [22] S.M. Parida, P.K. Rout, S.K. Kar, "An auxiliary control aided modified sliding mode control for a PMSG based wind energy conversion system," *World J. Eng.*, 16(6): 725-736, 2019.
- [23] N.M. Dehkordi, N. Sadati, M. Hamzeh, "A robust backstepping high-order sliding mode control strategy for grid-connected DG units with harmonic/interharmonic current compensation capability," *IEEE Trans. Sustainable Energy*, 8(2): 561-572, 2016.
- [24] J. Ritonja, D. Dolinar, B. Polajzer, "Adaptive and robust controls for static excitation systems," *Compel: Int. J. Comput. Math. Electr. Electron. Eng.*, vol. 34(3): 864-881, 2015.
- [25] R.P. Vieira, L.T. Martins, J.R. Massing, M. Stefanello, "Sliding mode controller in a multiloop framework for a grid-connected VSI with LCL filter," *IEEE Trans. Ind. Electron.*, 65: 4714-4723, 2017.
- [26] A. Zakipour, S. Shokri Kojori, M. Tavakoli Bina, "Closed-loop control of the grid-connected Z-source inverter using hyper-plane MIMO sliding mode," *IET Power Electron.*, 10(15): 2229 – 2241, 2017.
- [27] U.K. Shinde, S.G. Kadwane, S.Gawande, M.J.B. Reddy, D. Mohanta, "Sliding mode control of single-phase grid-connected quasi-Z-source inverter," *IEEE Access*, 5: 10232-10240, 2017.
- [28] F. Sebaaly, H. Vahedi, H.Y. Kanaan, N. Moubayed, K. Al-Haddad, "Design and implementation of space vector modulation-based sliding mode control for grid-connected 3L-NPC inverter," *IEEE Trans. Ind. Electron.*, 63: 7854-7863, 2016.
- [29] F. Sebaaly, H. Vahedi, H.Y. Kanaan, N. Moubayed, K. Al-Haddad, "Sliding mode fixed frequency current controller design for grid-connected NPC inverter," *IEEE J. Emerging Sel. Top. Power Electron.*, 4: 1397-1405, 2016.
- [30] H. Makhamreh, M. Trabelsi, O. Kükrer, H. Abu-Rub, "An effective sliding mode control design for a grid-connected puc7 multilevel inverter," *IEEE Trans.Indu. Electron.*, 67: 3717-3725, 2019.
- [31] M. Mehrasa, E. Pouresmaei, M.F. Akorede, B.N. Jørgensen, J.P. Catalão, "Multilevel converter control approach of active power filter for harmonics elimination in electric grids," *Energy*, 84: 722-731, 2015.

Biographies



Negin Ghaffari received the B.Sc. Degree in Electrical Engineering from the Arak University of Technology (ArakUT), Arak, Iran, in 2018 and presently she is studying on M.Sc. Degree in Power electronics, Arak University of Technology (ArakUT), Arak, Iran. Her research interests include nonlinear control of the active power filters and grid connected inverters.



Adel Zakipour was born in Ardabil, Iran, in 1981. He received his Ph.D. degrees in Electrical Engineering from K.N.Toosi University of technology, Tehran, Iran, in 2017. Currently, he is an assistant professor in power electronics at department of electrical engineering, Arak university of technology. His research interests include design and control of the DC/DC and DC/AC converter, grid connected inverters and variable speed drive.



Mahdi Salimi was born in Ardabil, Iran, in 1979. He received his B.S. and M.S. degrees in Electrical Engineering from K.N.T University of Technology, Tehran, Iran, in 2000 and 2002, respectively, and his Ph.D. degree in Power Electronics from Science and Research Branch, Islamic Azad University, Tehran, Iran, in 2012. Dr. Salimi has joined university of Nottingham, UK as a research fellow from 2019-2020. Since 2003, he has been with Islamic Azad University, where he is currently assistant professor at the department of electrical engineering. His research interests include closed-loop control of power electronics converters, high gain DC-DC converters, grid-connected inverters, and renewable energy.

Copyrights

©2021 The author(s). This is an open access article distributed under the terms of the Creative Commons Attribution (CC BY 4.0), which permits unrestricted use, distribution, and reproduction in any medium, as long as the original authors and source are cited. No permission is required from the authors or the publishers.



How to cite this paper:

N. Ghaffari, A. Zakipour, M. Salimi, "State space modeling and sliding mode current control of the grid connected multi-level flying capacitor inverters," *J. Electr. Comput. Eng. Innovations*, 9(2): 215-228, 2021.

DOI: [10.22061/JECEI.2021.7626.412](https://doi.org/10.22061/JECEI.2021.7626.412)

URL: https://jecei.sru.ac.ir/article_1521.html

